

การศึกษาเชิงทฤษฎีของสเปกตรัมทะลุผ่านของรอยต่อของ  
โลหะ-ตัวนำยิ่งยวด-โลหะ

นางสาวอารีรัตน์ ดาวงษา

วิทยานิพนธ์นี้เป็นส่วนหนึ่งของการศึกษาตามหลักสูตรปริญญาวิทยาศาสตรมหาบัณฑิต  
สาขาวิชาฟิสิกส์  
มหาวิทยาลัยเทคโนโลยีสุรนารี  
ปีการศึกษา 2552

**THEORETICAL STUDY OF TUNNELING  
SPECTROSCOPY OF METAL-SUPERCONDUCTOR-  
METAL JUNCTIONS**

**Areerat Dawongsa**

**A Thesis Submitted in Partial Fulfillment of the Requirements for  
the Degree of Master of Science in Physics  
Suranaree University of Technology  
Academic Year 2009**

**THEORETICAL STUDY OF TUNNELING SPECTROSCOPY OF  
METAL-SUPERCONDUCTOR-METAL JUNCTIONS**

Suranaree University of Technology has approved this thesis submitted in partial fulfillment of the requirements for the Degree of Master of Science

Thesis Examining Committee

---

(Asst. Prof. Dr. Chinorat Kobdaj)

Chairperson

---

(Assoc. Prof. Dr. Puangratana Pairor)

Member (Thesis Advisor)

---

(Assoc. Prof. Dr. Prapun Manyum)

Member

---

(Dr. Khanchai Khosonthongkee)

Member

---

(Prof. Dr. Sukit Limpijumnong)

Vice Rector for Academic Affairs

---

(Assoc. Prof. Dr. Prapun Manyum)

Dean of Institute of Science

อารีรัตน์ ดาวงษา : การศึกษาเชิงทฤษฎีของสเปกตรัมทะลุผ่านของรอยต่อของโลหะ-  
ตัวนำยวดยิ่ง-โลหะ (THEORETICAL STUDY OF TUNNELING SPECTROSCOPY OF  
METAL-SUPERCONDUCTOR-METAL JUNCTIONS)

อาจารย์ที่ปรึกษา : รองศาสตราจารย์ ดร.พวงรัตน์ ไพเราะ, 37 หน้า.

วิทยานิพนธ์นี้เป็นการศึกษาเชิงทฤษฎีของสเปกตรัมทะลุผ่านของรอยต่อโลหะ-ตัวนำยวดยิ่ง-โลหะในสองมิติ ในการศึกษานี้ได้พิจารณาตัวนำยวดยิ่งแบบเอส-เวฟ (ไอโซทรอปิก) และแบบดี-เวฟ (แอนไอโซทรอปิก) โดยใช้วิธีการกระจงในการคำนวณหาค่าสภาพความนำไฟฟ้าที่เป็นฟังก์ชันของความต่างศักย์ตกคร่อมระบบที่อุณหภูมิศูนย์องศาสัมบูรณ์ สมบัติที่แปรเปลี่ยนได้หลายตัวซึ่งมีผลต่อสเปกตรัมของสภาพความนำไฟฟ้าจะถูกศึกษา ซึ่งรวมไปถึงปัจจัยดังต่อไปนี้ คือ ผลของความหนาของชั้นตัวนำยวดยิ่ง ความสูงของพลังงานของกำแพงศักย์ที่บริเวณรอยต่อทั้งสอง และผลของการวางตัวของผลึกของตัวนำยวดยิ่งเทียบกับรอยต่อ

ความหนาของชั้นตัวนำยวดยิ่งเป็นตัวควบคุมขนาดของค่าสภาพความนำไฟฟ้าในลักษณะที่เห็นได้เด่นชัดซึ่งเป็นที่เข้าใจเป็นอย่างดี เนื่องจากการแทรกสอดของคลื่นจากขอบเขตของรอยต่อทั้งสองข้างของชั้นตัวนำยวดยิ่ง ซึ่งการแกว่งกวัดของสภาพความนำไฟฟ้านี้จะขึ้นกับชั้นของความหนา ซึ่งเรียกว่า การแกว่งกวัดแบบโทมัส

ในคำนวณสเปกตรัมสภาพนำไฟฟ้าของเรา เราทำซ้ำการแกว่งกวัดแบบโทมัสและเราเน้นที่จะระบุว่าผลของการเปลี่ยนแปลงค่าความสูงของพลังงานของกำแพงศักย์ที่บริเวณรอยต่อทั้งสองมีผลอย่างไรต่อการกวัดแกว่งโทมัส เราระบุได้ว่าทั้งและลักษณะเชิงคุณภาพของสภาพความนำไฟฟ้ารวมทั้งการกวัดแกว่งโทมัสขึ้นอยู่กับความสูงของกำแพงศักย์บริเวณรอยต่อด้านซ้ายมือและขวามือ (ในการศึกษานี้ พาหะประจุบวกจะเห็นกำแพงศักย์ทางด้านซ้ายมือสูงกว่าเมื่อมีการให้ความต่างศักย์เป็นบวก) อิเล็กตรอนถูกยิงเข้าไปในตัวนำยวดยิ่งจากโลหะทางด้านซ้ายมือ ในขณะที่โฮลถูกยิงจากโลหะทางด้านขวามือ (พาหะประจุตรงกันข้ามจะต้องถูกยิงออกมาในเวลาเดียวกันเข้าสู่ตัวนำยวดยิ่งเพื่อให้เกิดการอนุรักษ์ของกระแสไฟฟ้า) ด้วยเหตุนี้กำแพงศักย์ด้านซ้ายมือจึงสะท้อนอิเล็กตรอนออกมาส่วนทางด้านขวามือของรอยต่อจึงสะท้อนโฮลออกมา

หนึ่งในผลการศึกษาที่สำคัญอย่างหนึ่งในงานวิจัยนี้คือ ความสำคัญเชิงสัมพัทธ์ของความสูงกำแพงศักย์เปลี่ยนแปลงไปกับค่าความต่างศักย์ตกคร่อมระบบ ทั้งกรณีของตัวนำยวดยิ่งแบบเอส-เวฟ และแบบดี-เวฟ เราพบว่ากำแพงศักย์ด้านซ้าย (อิเล็กตรอน) มีอิทธิพลต่อสภาพความนำไฟฟ้าตลอดช่วงของความต่างศักย์ตกคร่อม ในขณะที่กำแพงศักย์ทางด้านขวามือ (โฮล)

มีผลกระทบต่อสภาพความนำไฟฟ้าเมื่อความต่างศักย์ตกคร่อมมีค่ามากกว่าช่องว่างพลังงานสูงสุดของตัวนำยวดยิ่ง

แอนไอโซทรอปีของตัวนำยวดยิ่งแบบดี-เวฟ ทำให้รอยต่อโลหะ-ตัวนำยวดยิ่ง-โลหะที่มีตัวนำยวดยิ่งแบบดีเวฟเป็นส่วนประกอบมีความไวต่อทิศทางการวางตัวของผลึกตัวนำยวดยิ่ง ลักษณะของสเปกตรัมของสภาพความนำไฟฟ้าสะท้อนความเป็นแอนไอโซทรอปีของค่าช่องว่างพลังงาน ตัวอย่างเช่น ยอดสูงที่ค่าความต่างศักย์ตกคร่อมมีค่าเป็นศูนย์ในสเปกตรัมสภาพความนำไฟฟ้าเกิดขึ้นเมื่อทิศทางของโมเมนต์ของช่องว่างพลังงานต่ำสุดขนานกับทิศที่ตั้งฉากผิวรอยต่อ ความสูงและความกว้างของยอดมีค่าลดลงเมื่อผลึกมีทิศทางการหมุนการวางตัวดังกล่าว และหายไปอย่างสมบูรณ์เมื่อทิศทางของค่าช่องว่างพลังงานที่สูงสุดตรงกับทิศที่ตั้งฉากกับระนาบของรอยต่อ

AREERAT DAWONGSA : THEORETICAL STUDY OF TUNNELING  
SPECTROSCOPY OF METAL-SUPERCONDUCTOR-METAL  
JUNCTIONS. THESIS ADVISOR : ASSOC. PROF. PUANGRATANA  
PAIROR, Ph.D. 37 PP.

THEORETICAL STUDY OF TUNNELING SPECTROSCOPY OF METAL-  
SUPERCONDUCTOR-METAL JUNCTIONS

This thesis is a theoretical study the tunneling spectroscopy of metal-superconductor-metal double junctions (MSM) composed of two dimensional electronic materials. In this study, we considered two types of superconductors: those having s-wave (i.e. isotropic) and d-wave (anisotropic) gap symmetries. The zero-temperature differential conductance was calculated by a scattering method. Several variable properties of junctions that affect the conductance spectrum have been studied. These include: the thickness of superconducting layer, the barrier height at both interfaces and the superconducting crystal orientation relative to the interface.

The thickness of the superconducting layer controls the magnitude of the conductance in a distinctive manner that is well understood. Because of the interference of waves scattered from the two boundaries of the superconducting layer, there is an oscillatory dependence of the conductance on the layer thickness, the so called Tomasch oscillations.

Having reproduced the Tomasch oscillations in our calculation, our focus was to determine how these oscillations are affected by a variation in the relative barrier heights at the two metal-superconductor interfaces. We determined that both the

magnitude of the conductance and the qualitative spectral features, including the Tomasch oscillations, depend on the left and right barrier heights. (In our convention, a positive charge carrier sees a higher potential at the left barrier when the applied voltage is positive.) Electrons are injected into the superconductor from the metal on the left while holes are injected from the metal on the right (opposite charge carriers must be simultaneously injected into the superconductor to ensure current conservation). Therefore the left barrier scatters incoming electrons while the right barrier scatters incoming holes.

One of the remarkable results of this thesis is that the relative importance of the two barriers changes with the applied voltage. In both s-wave and d-wave superconducting junctions, we found that the left (electron) barrier influences the conductance throughout the range of the applied voltage, whereas the right (hole) barrier only affects the conductance when the applied voltage is larger than the maximum gap.

The anisotropy of a d-wave superconductor makes MSM junctions involving it sensitive to crystal orientation. The qualitative spectral features of the conductance reflect this gap anisotropy. For example, a broad peak in the conductance at zero voltage occurs when the momentum direction of the gap minimum is parallel to the surface normal. The height and width of this peak decreases as the crystal is rotated away from this orientation and the peak vanishes completely when the interface normal coincides with the direction of the gap maximum.

School of Physics

Student's Signature \_\_\_\_\_

Academic Year 2009

Advisor's Signature \_\_\_\_\_

## **ACKNOWLEDGEMENTS**

The first person, I would like to express my gratitude to, is Ajarn Paungratana, my thesis advisor for her invaluable suggestions and encouragement she had given to me throughout this research. I also wish to thank Asst. Prof. Dr. Chinorat Kobdaj, Assoc. Prof. Dr. Prapun Manyum, and Dr. Khanchai Khosonthongkee for being on my supervisory thesis committee, and also for helpful comments and suggestions on thesis writing.

Thank you to all members in Physics group for their help and useful discussions, especially, Dr. Benjamat Srisongmuang, Mr. Rarm Phinjaroenphan, Mr. Krisakron Pasanai, Mr. Aek Jantayod, Miss Achara Ka-oey, and Dr. Ayut Liphirat.

I am also grateful for the Commission on Higher Education for the financial support in my last two years of the research.

Finally, I would like to express my deep gratitude to my father, Mr. Veerayut Dawongsa, my mother, Mrs. Srisuda Dawongsa, and all members in my family for their constant loving support.

Areerat Dawongsa



# CONTENTS

	<b>Page</b>
ABSTRACT IN THAI.....	I
ABSTRACT IN ENGLISH.....	III
ACKNOWLEDGEMENTS.....	V
CONTENTS .....	VI
LIST OF FIGURES .....	VII
<b>CHAPTER</b>	
<b>I INTRODUCTION.....</b>	<b>1</b>
1.1 Background and motivation.....	1
1.2 Assumptions and method of calculation.....	2
1.3 Outline of thesis .....	8
<b>II METHOD OF CALCULATION.....</b>	<b>9</b>
<b>III CONDUCTANCE SPECTRA OF MSM JUNCTIONS.....</b>	<b>21</b>
3.1 The effect of the thickness of superconducting layer .....	21
3.2 The effect of insulating barrier potentials.....	25
3.3 The effect of the crystal orientation of d-wave superconductor .....	30
<b>IV CONCLUSIONS .....</b>	<b>31</b>
REFERENCES .....	35
CURRICULUM VITAE.....	37

## LIST OF FIGURES

Figure	Page
<p>1.1 On the left is the crystal structure of <math>\text{YBa}_2\text{Cu}_3\text{O}_{7-x}</math> (YBCO), lattice constants of which are <math>a = 3.82 \text{ \AA}</math>, <math>b = 3.89 \text{ \AA}</math>, and <math>c = 11.6802 \text{ \AA}</math>, and on the right is the crystal structure of <math>\text{La}_{2-x}\text{Sr}_x\text{CuO}_4</math> (LSCO) with lattice constants <math>a = b = 3.78 \text{ \AA}</math>, and <math>c = 13.18 \text{ \AA}</math> .....</p>	2
<p>1.2 Diagram of the geometry of an MSM junctions. Both metals occupy the spaces where <math>x &lt; 0</math>, <math>x &gt; L</math> and the superconductor occupies the space where <math>0 &lt; x &lt; L</math>. The two insulating layers at <math>x = 0</math> and <math>x = L</math>, which are represented by delta-function barrier potentials of height <math>H_1</math> and <math>H_2</math>, <math>L</math> is the thickness of superconductor, <math>\Delta_k</math> is the superconducting gap .....</p>	6
<p>2.1 The sketches of the geometry of MSM junctions. Both metals occupy the spaces where <math>x &lt; 0</math>, <math>x &gt; L</math> and the superconductor occupies the space where <math>0 &lt; x &lt; L</math>. The two insulating layers at <math>x = 0</math> and <math>x = L</math>, which are represented by delta-function barrier potentials of height <math>H_1</math> and <math>H_2</math>, <math>L</math> is the thickness of superconductor .....</p>	9

## LIST OF FIGURES (Continued)

<b>Figure</b>	<b>Page</b>
2.2 The sketches of two types of superconducting gaps in the momentum space. The black circles represent the Fermi spheres. The solid lines represent the minimum energy contour of the excitations in an s-wave superconductor (left) and a d-wave superconductor (right). The plus and minus signs represent the phase of the gap .....	11
2.3 The sketch of the energy dispersion relation and the indications of the excitation states participating in the incoming and reflecting off the interface on the left side of an MSM junction, in the case where an electron is injected from the left. The solid curves represent the electron excitation spectrum and the dashed curves represent the hole excitation spectrum. The black (●) and white (○) dots represent electron and hole excitations that involve the incoming and reflection surface .....	13
2.4 Schematic illustration of the energy dispersion relation in the superconductor region. The black and white dot represent electron-like and hole-like quasiparticle excitations of the same energy .....	14

## LIST OF FIGURES (Continued)

<b>Figure</b>	<b>Page</b>
2.5    The diagram of the excitation energy dispersion relation of the particles in the metal on the right. The black and white dots represent the transmitted excited electron and excited hole in the case where an electron is injected from the left side respectively.....	16
3.1    The conductance as a function of applied voltage ( $eV / \Delta_0$ ) for three different thicknesses of the s-wave superconducting layer ( $Lk_F$ ):  (a) $Lk_F = 500$ , (b) $Lk_F = 1000$ , and (c) $Lk_F = 1500$ . Here, $\Delta_0 / E_F = 0.01$ and $Z_1 = Z_2 = 1.0$ . The solid upright lines represent the positions of the minima of the oscillations in the conductance spectra.....	22
3.2    The conductance as a function of applied voltage ( $eV / \Delta_0$ ) for three different thicknesses of the d-wave superconducting layer ( $Lk_F$ ):  (a) $Lk_F = 500$ , (b) $Lk_F = 1000$ , and (c) $Lk_F = 1500$ . Here, $\Delta_0 / E_F = 0.01$ , $Z_1 = Z_2 = 1.0$ , and $\alpha = 0$ . The solid upright lines represent the positions of the minima of the oscillations in the conductance spectra.....	23

## LIST OF FIGURES (Continued)

<b>Figure</b>	<b>Page</b>
3.2 The conductance as a function of applied voltage ( $eV / \Delta_0$ ) for three different thicknesses of the d-wave superconducting layer ( $Lk_F$ ):  (a) $Lk_F = 500$ , (b) $Lk_F = 1000$ , and (c) $Lk_F = 1500$ . Here, $\Delta_0 / E_F = 0.01$ , $Z_1 = Z_2 = 1.0$ , and $\alpha = 0$ . The solid upright lines represent the positions of the minima of the oscillations in the conductance spectra. (Continued).....	24
3.3 The conductance spectra of MSM junctions with the different values of $Z_1$ and $Z_2$ . Here, we take $\Delta_0 / E_F = 0.01$ and $Lk_F = 1000$ : (a) s-wave case and (b) d-wave case .....	26
3.4 The conductance spectra of s-wave superconductor with different values of $Z_2$ . We take $\Delta_0 / E_F = 0.01$ , $Lk_F = 1000$ , and $Z_1 = 0.5$ .....	27
3.5 The conductance spectra of d-wave superconductor with different values of $Z_2$ . We take $\Delta_0 / E_F = 0.01$ , $Lk_F = 1000$ , $\alpha = 0$ , and $Z_1 = 0.5$ .....	28

## LIST OF FIGURES (Continued)

<b>Figure</b>	<b>Page</b>
<p>3.6 The conductance spectra of s-wave superconductor with different values of <math>Z_2</math>. We take <math>\Delta_0 / E_F = 0.01</math>, <math>Lk_F = 1000</math>, and <math>Z_2 = 0.7</math> .....</p>	29
<p>3.7 The conductance spectra of d-wave superconductor with different values of <math>Z_2</math>. We take <math>\Delta_0 / E_F = 0.01</math>, <math>Lk_F = 1000</math>, <math>\alpha = 0</math>, and <math>Z_2 = 0.7</math> .....</p>	29
<p>3.8 The conductance spectra of d-wave junctions with different values of <math>\alpha : 0, \pi / 8, \pi / 6</math>, and <math>\pi / 4</math>. We take <math>\Delta_0 / E_F = 0.01</math> and <math>Z_1 = Z_2 = 1</math> .....</p>	30

# CHAPTER I

## INTRODUCTION

### 1.1 Background and motivation

In a double junction, a structure consisting of three layers of materials, particle waves moving to the left and to the right can interfere. The interference causes the particle transmission probability through the junction to oscillate with the particle energy. In general, the period of the oscillation depends on the thickness and the physical properties of the middle layer (Shankar, 1994). One can observe the interference by measuring the current-voltage characteristics, or alternatively the conductance spectrum the first derivatives of the current with respect to the applied voltage *vs* the applied voltage of the double junction. In principle, one can extract information about an unknown material by studying these properties of a junction when the unknown material is in the middle. In this thesis, the materials of interest include conventional and high-temperature superconductors.

Superconductors have remarkable properties. They are perfect diamagnets and perfect conductors. Most metals can become superconducting at very low temperatures, well below 77 K the boiling point of liquid nitrogen (Marder, 2000). In the ground state, the electrons in a superconductor are paired in bound states called Cooper pairs. For most conventional superconductors like Indium (In), Aluminum (Al), Lead (Pb), and Niobium-titanium (NbTi), the mechanism that binds electrons in Cooper pairs is an attraction due to the electron-phonon coupling, which dominates

the Coulomb repulsion and electron kinetic energy at sufficiently low temperature. The minimum energy needed to break a Cooper pair is called the superconducting gap. The superconducting gap of a conventional superconductor is approximately momentum-independent, i.e. the same for all wave vectors  $\vec{k}$ , and is called isotropic s-wave. Certain unconventional superconductors exhibit different superconducting gap symmetries. High temperature superconductors are ceramic compounds consisting of at least one copper oxide plane, and are one of the most studied materials in existence (see Figure 1.1).

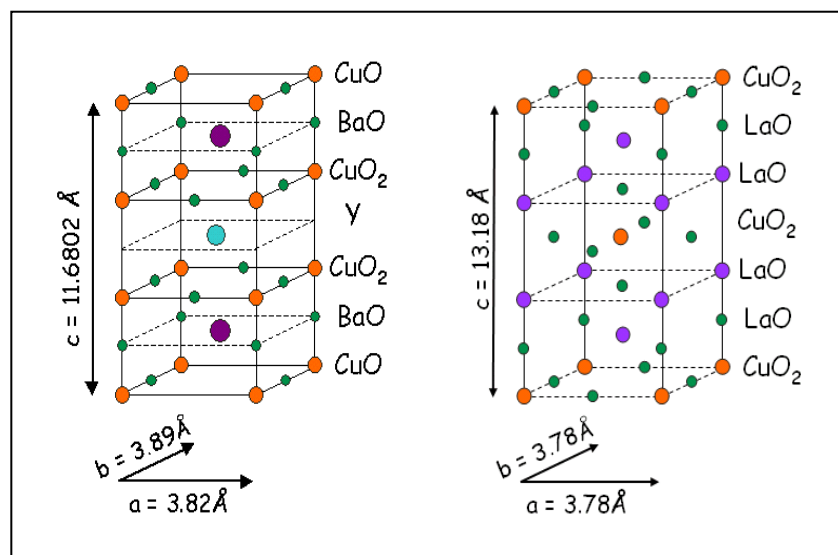


**Figure 1.1** On the left is the crystal structure of  $\text{YBa}_2\text{Cu}_3\text{O}_{7-x}$  (YBCO), lattice constants of which are  $a = 3.82 \text{ \AA}$ ,  $b = 3.89 \text{ \AA}$ , and  $c = 11.6802 \text{ \AA}$ , and on the right is the crystal structure of  $\text{La}_{2-x}\text{Sr}_x\text{CuO}_4$  (LSCO) with lattice constants  $a = b = 3.78 \text{ \AA}$ , and  $c = 13.18 \text{ \AA}$ . (<http://hoffman.physics.harvard.edu/materials/Cuprates.php>).



The electrical conduction along the copper oxide planes can be orders of magnitude higher than that perpendicular to the planes (Tsuei and Kirtley, 2000). Therefore, one can model these materials as two dimensional (2D) systems. The superconducting gaps of these materials are found to be strongly momentum-dependent within the 2D plane. They are  $d_{x^2-y^2}$ -wave (that is they are functions that have the same symmetry in momentum space as the function  $k_x^2 - k_y^2$ ). The gap magnitude goes to zero for wave vectors along the diagonals  $k_x = \pm k_y$  and has opposite sign on opposite sides of these diagonals.

In this masters thesis, a metal-superconductor-metal (MSM) double junction will be theoretically studied. Two types of superconductors are considered: isotropic s-wave and d-wave. The superconducting layer in an MSM junction causes oscillations in the electrical conductance spectrum. These oscillations called Tomasch oscillations after Tomasch, who measured the resistivity as a function of applied voltage of Al-Al<sub>2</sub>O<sub>3</sub>-Pb junction with variable Pb thicknesses between 2.9 to 9.7 microns (Tomasch, 1965). The junction was cooled down below the superconducting transition temperature of Pb. He found that the relation between the first derivative of the voltage with respect to the current exhibited oscillations. The distance between the two adjacent peaks of oscillations is inversely proportional to the thickness of Pb (Tomasch, 1965). He also measured the resistivity spectrum of a similar junction with In as a superconducting layer and obtained similar results (Tomasch, 1966; Tomasch and Wolfram, 1966). The oscillating behavior was first explained by McMillan and Anderson in to be due to quasiparticle interference in the superconducting layer (McMillan and Anderson, 1966). They showed that the oscillation period depends on

the thickness ( $L$ ), the Fermi velocity ( $v_F$ ), and the energy gap ( $\Delta_k$ ) of the superconducting layer (McMillan and Anderson, 1966):

$$E_n = \sqrt{\Delta_k^2 + \left(\frac{\pi n \hbar v_F}{L}\right)^2}, \quad (1.1)$$

where  $E_n$  is the position of each oscillation peak,  $n$  is an integer. By considering the Tomasch oscillations, one can therefore extract this information about the superconducting layer. The Tomasch oscillations can potentially be used to detect the gap anisotropies of anisotropic superconductors, like anisotropic s-wave and d-wave superconductors, as well. Lykken and his colleagues used the Tomasch oscillation to measure the anisotropy of the superconducting gap and the Fermi velocity of Pb along several crystal orientations such as [100], [110], [111], and [211] (Lykken, Geiger, Dy, and Mitchell, 1970; Lykken, Geiger, Dy, and Mitchell, 1971). As for the case of d-wave superconductors, one of the experimental work was done by Koren and his colleagues. They measured the Tomasch oscillations of YBCO film and found its energy gap and its Fermi velocity (Koren, Polturak, and Deutscher, 1996; Neshor and Koren, 1999).

There has not also been much theoretical study of the Tomasch oscillations in a d-wave superconductor. Dong and his colleagues used the scattering method to study a metal-d-wave superconductor-metal junction. They calculated the conductance spectrum of the junction in two orientations. In one of the orientations, the direction of the gap maximum is oriented perpendicular to the interface planes. In another orientation the direction of the gap maximum is pointing  $45^\circ$  from the

interface planes. In their calculation, they assumed the two metals are identical and the insulating barriers at both interfaces are the same (Dong, Zheng, and Xing, 2004).

In this thesis, the Tomasch oscillations of two-dimensional (2D) isotropic s-wave superconductors and d-wave superconductors will be considered. The effects of the unequal insulating barriers and in the d-wave case the effect of the crystal orientation of the superconductor will also be considered. The superconducting gap is not constant and the crystal orientation of the d-wave superconducting plane other than the plane [100] and [110] gives a different phase angle. Except the case of [100] plane we have found the characteristic energy is equal to zero and gradually decrease until a specific level of energy. This feature is called zero-bias conductance peak (ZBCP) (Tanaka and Kashiwaya, 1995). From most of the studies, the junction is a single junction. For the study of the double junctions, it is found that they only considered two planes of crystal orientation of the superconductor, [100] and [110].

## 1.2 Assumptions and method of calculation

In this thesis, all MSM junctions are modeled as 2D infinite systems occupying the  $xy$  plane. The two metals occupy the  $x < 0$  and  $x > L$  regions and a superconducting layer is in between (as shown in Figure 1.2). The superconducting gap is taken to be position-independent, but can depend on the wave vector especially for a d-wave superconductor. Both interfaces are assumed to be smooth; so that, the component parallel to the surface of the momentum of the quasiparticle in each region is conserved.

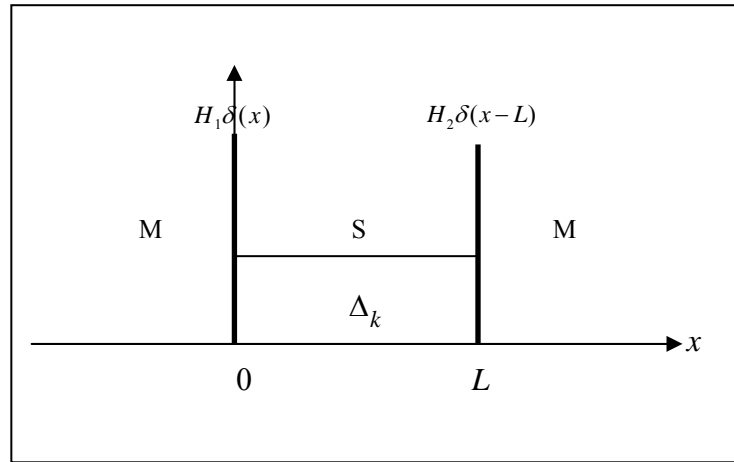


**Figure 1.2** Diagram of the geometry of an MSM junctions. Both metals occupy the spaces where  $x < 0$ ,  $x > L$  and the superconductor occupies the space where  $0 < x < L$ . The two insulating layers at  $x = 0$  and  $x = L$ , which are represented by delta-function barrier potentials of height  $H_1$  and  $H_2$ ,  $L$  is the thickness of superconductor,  $\Delta_k$  is the superconducting gap.

The method used in this thesis is based on a scattering method analogous to that used in undergraduate quantum mechanics courses. This scattering formalism is a simple approach and now one of the formalisms widely used to study the particle transport in a heterostructure. It was first used by Blonder, Tinkham, and Klapwijk (Blonder, Tinkham, and Klapwijk, 1982) to calculate the current and conductance spectra of a metal-superconductor junction and is thus sometimes referred to as the BTK formalism. The starting point is to write down the Hamiltonian describing the junction in a free electron approximation. In this approximation, the energy dispersion relation of electrons in a conduction band of a metal is parabolic. On the superconducting side, the excitation energy in this approximation is

$$E_k = \sqrt{\left(\frac{\hbar^2 k^2}{2m} - E_{FS}\right)^2 + \Delta_k^2},$$

where  $m$  is the mass of the electron,  $\vec{k}$  is the wave vector,  $E_{FS}$  is the Fermi energy of the superconductor, and  $\Delta_k$  is the superconducting gap, which in case of a s-wave superconductor is taken to be  $\Delta_k = \Delta_0$ , where  $\Delta_0$  is a constant, and in case of a d-wave superconductor is taken to be  $\Delta_k = \Delta_0 \cos 2(\theta_k - \alpha)$ , where  $\theta_k$  is the angle between the wave vector and the left interface normal, and  $\alpha$  is the angle between the  $a$ -axis of the superconductor and the left interface normal (so the argument of the cosine describes the direction of  $\vec{k}$  relative to the crystal axis and results in a gap that has maximum magnitude along the square axes and vanishes along the diagonal). The gap is set to be zero in the normal metal and is assumed to be position-independent in the superconductor for simplicity (see Figure 1.2), i.e. we neglect the proximity effects. The insulating layers at both interfaces are represented by the delta-function barrier potentials  $H_1\delta(x)$  and  $H_2\delta(x-L)$ , respectively.

According to the work of Dong, Zheng, and Xing (2004), we consider the injection of the electron and hole together by injecting electrons from metal to the left and right side. We need to inject both electron and hole into the system in order to conserve electric current within the system. In this study, we calculate conductance of the junctions at zero temperature using the elastic scattering method.

### **1.3 Outline of research**

In this thesis, we consider MSM junctions, involving s-wave and d-wave superconductors. Our main focus is on the effect of interface quality on the conductance spectra of both types of junctions. For a d-wave superconductor junction, we also consider the influence of the superconducting crystal orientation on the spectrum. In the next chapter, we will present the method we use to calculate the conductance spectra of MSM junctions. We present the results for both s-wave and d-wave superconductor junctions in Chapter III. We finally provide a summary of main results and conclude in Chapter IV.

## CHAPTER II

### METHOD OF CALCULATION

In this chapter, the method used to calculate the conductance spectra of MSM junctions is presented. In this method, each of our junctions is represented by an infinite two-dimensional system, where a superconductor of thickness  $L$  is sandwiched by two identical metals. At each interface, we assign a delta-function potential to depict an insulating layer. We use a free electron model to describe the electronic properties of each region.

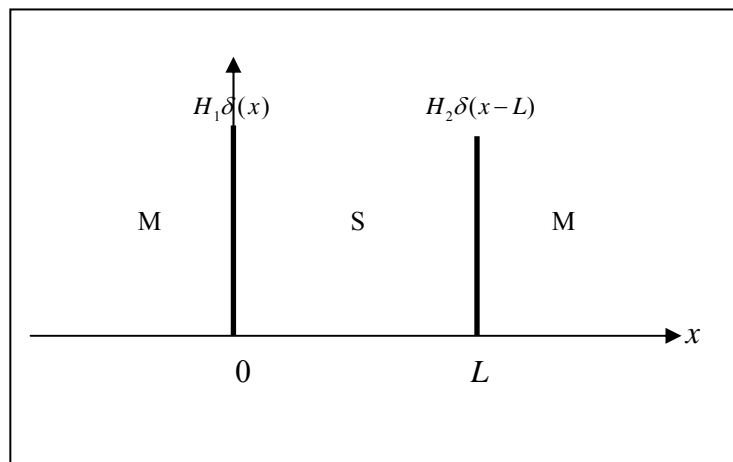


**Figure 2.1** The sketches of the geometry of MSM junctions. Both metals occupy the spaces where  $x < 0$ ,  $x > L$  and the superconductor occupies the space where  $0 < x < L$ . The two insulating layers at  $x = 0$  and  $x = L$ , which are represented by delta-function barrier potentials of height  $H_1$  and  $H_2$ ,  $L$  is the thickness of superconductor.

We follow the approach used by Griffin and Demers and also by Blonder, Tinkham, and Klapwijk (Griffin and Demers, 1971; Blonder, Tinkham, and Klapwijk, 1982) to calculate the current and conductance spectra of our junctions. In this approach, the junction is described by the Bogoliubov de Gennes (BdG) equations:

$$\begin{bmatrix} H(x, y) & \Delta(x, y) \\ \Delta^*(x, y) & -H(x, y) \end{bmatrix} \psi(x, y) = E \psi(x, y) \quad (2.1)$$

Where  $H = \left( -\frac{\hbar^2 \nabla^2}{2m} \right) + V(x) - E_{FL} \Theta(-x) - E_{FS} (\Theta(x) - \Theta(x-L)) - E_{FR} \Theta(x-L)$  is the Hamiltonian of an MSM junction and  $\Delta(x) = \Delta_k (\Theta(x) - \Theta(x-L))$ .  $L$  is the thickness of superconducting layer.  $\Theta(x)$  is the Heaviside step function.  $E_{FL}$  and  $E_{FR}$  are the Fermi energies of the metal on the left and right hand side, respectively. Because we take both metals to be identical,  $E_{FL} = E_{FR}$ .  $E_{FS}$  is the Fermi energy of the superconductor.  $V(x) = H_1 \delta(x) + H_2 \delta(x-L)$  is the insulating barrier potentials located at both interfaces.  $H_1$  and  $H_2$  can take different values.  $\Delta_k$  is the superconducting gap. In this thesis, we consider two types of superconductors, s-wave and d-wave superconductors. For s-wave superconductors, the superconducting gap is taken to be independent of the wave vector:  $\Delta_k = \Delta_0$ , where  $\Delta_0$  is a constant. For d-wave superconductors, the gap is taken to be  $\Delta_k = \Delta_0 \cos 2(\theta_k - \alpha)$ , where  $\theta_k$  is the angle between the wave vector and the interface normal (the  $x$ -axis in Figure 2.1).  $\alpha$  is the angle between the  $a$ -axis of the superconductor and the interface normal.



$\psi(x, y)$  is the two-component wave function  $\psi(x, y) = \begin{pmatrix} u_k \\ v_k \end{pmatrix} e^{ik_x x} e^{ik_y y}$ , where  $u_k$  and  $v_k$

are electron-like and hole-like quasiparticle amplitudes defined as follows:

$$u_k = \frac{E + \xi_k}{\sqrt{|E + \xi_k|^2 + |\Delta_k|^2}} \quad \text{and} \quad v_k = \frac{\Delta_k}{\sqrt{|E + \xi_k|^2 + |\Delta_k|^2}} \quad \text{where} \quad \xi_k = \sqrt{E_k^2 - \Delta_k^2}. \quad E \text{ is the}$$

energy of an excitation.

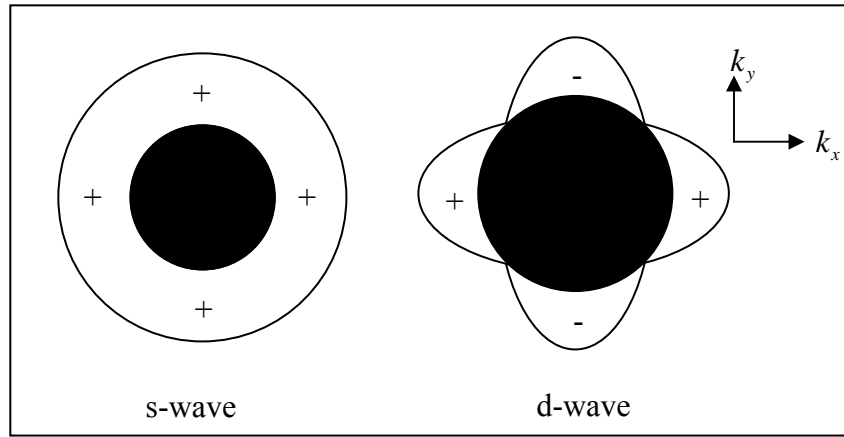


**Figure 2.2** The sketches of two types of superconducting gaps in the momentum space. The black circles represent the Fermi spheres. The solid lines represent the minimum energy contour of the excitations in an s-wave superconductor (left) and a d-wave superconductor (right). The plus and minus signs represent the phase of the gap.

From the BdG equations, the excitation energy spectrum and the corresponding eigenfunction in each region can be obtained. For the metal on the left side ( $x < 0$ ), the energy spectra for electron and hole excitations are

$$E_{ML} = \pm \frac{\hbar^2 (q_L^2 + q_y^2)}{2m} \mp E_{FL} \quad (2.2)$$

where the plus and minus signs are for electron and hole excitations, respectively.

We consider two cases of particle injection: an injection of an electron from the left metal and that of hole from the right metal. The particle transmission probabilities in both cases are needed for the calculation of the conductance; so that the electric current is conserved in every plane of consideration (Dong, Zheng, and Xing, 2004).

In the first case, the involving excited states of the electrons in the left metal are shown in Figure 2.3. Andreev and normal reflection coefficients are denoted by  $(r_h)$  and  $(r_e)$  in the figure. In the superconductor, electron-like and hole-like quasiparticle reflection coefficients are denoted by  $(c_2)$  and  $(d_2)$ , and electron-like and hole-like transmission coefficients are denoted by  $(c_1)$  and  $(d_1)$  (as shown in Figure 2.4). In the left excited electron and excited hole transmission coefficients are denoted by  $(t_e)$  and  $(t_h)$  (as shown in Figure 2.5). In the second case of the injection, one can figure similar states that are involved.

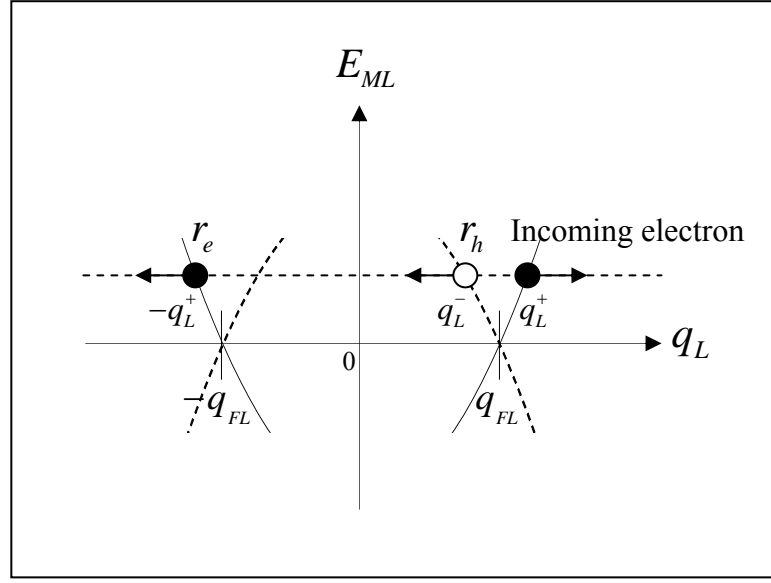


**Figure 2.3** The sketch of the energy dispersion relation and the indications of the excitation states participating in the incoming and reflecting off the interface on the left side of an MSM junction, in the case where an electron is injected from the left. The solid curves represent the electron excitation spectrum and the dashed curves represent the hole excitation spectrum. The black (●) and white (○) dots represent electron and hole excitations that involve the incoming and reflection surface.

The wave functions of the particle excitations in the left metal in both cases are

$$\psi_{ML(e)}(x, y) = \left( \begin{pmatrix} 1 \\ 0 \end{pmatrix} e^{iq_L^+ x} + r_h \begin{pmatrix} 0 \\ 1 \end{pmatrix} e^{iq_L^- x} + r_e \begin{pmatrix} 1 \\ 0 \end{pmatrix} e^{-iq_L^+ x} \right) e^{ik_y y} \quad (2.3)$$

$$\psi_{ML(h)}(x, y) = \left( \begin{pmatrix} -1 \\ t_e \end{pmatrix} e^{-iq_L^+ x} + \begin{pmatrix} 0 \\ t_h \end{pmatrix} e^{iq_L^- x} \right) e^{ik_y y} \quad (2.4)$$

where the wave functions with subscript  $e$  and  $h$  are for the case where an electron is injected from the left and where a hole is injected from the right, respectively.  $r_h$  and

$r_e$  are the Andreev and normal reflection coefficients, respectively.  $\bar{t}_e$  and  $\bar{t}_h$  are the electron-like and hole-like quasiparticle transmission coefficients, respectively.  $q_L^+$  and  $q_L^-$  are the  $x$ -component of the wave vectors for excited electron and hole, respectively.

For the superconductor region ( $0 < x < L$ ), the excitation energy spectrum are

$$E_S = \sqrt{\left(\frac{\hbar^2(k^2 + k_y^2)}{2m} \mp E_{FS}\right)^2 + \Delta_k^2} \quad (2.5)$$

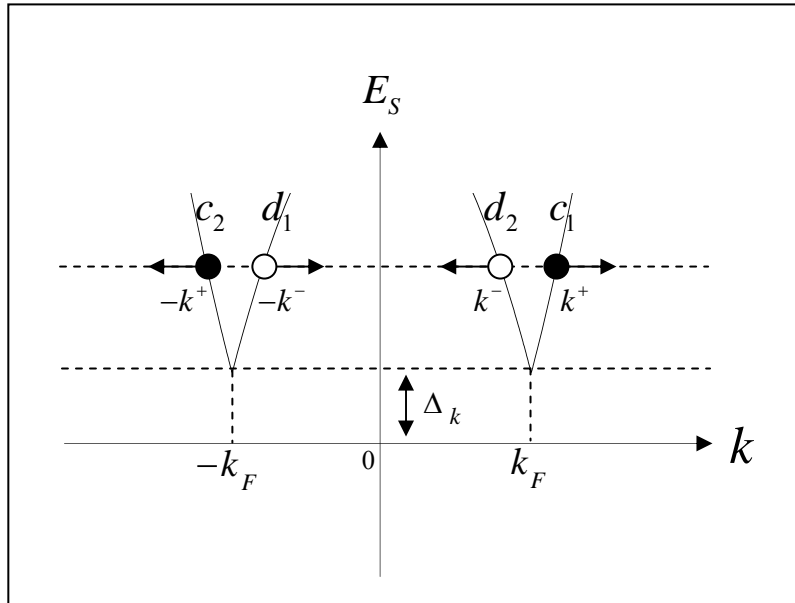


**Figure 2.4** Schematic illustration of the energy dispersion relation in the superconductor region. The black and white dots represent electron-like and hole-like quasiparticle excitations of the same energy.

The wave functions of the excitations in the superconducting layer in both cases are

$$\psi_{S(e)}(x, y) = \left( c_1 \begin{pmatrix} u_{k^+} \\ v_{k^+} \end{pmatrix} e^{ik^+x} + d_1 \begin{pmatrix} u_{-k^-} \\ v_{-k^-} \end{pmatrix} e^{-ik^-x} + c_2 \begin{pmatrix} u_{-k^+} \\ v_{-k^+} \end{pmatrix} e^{-ik^+x} + d_2 \begin{pmatrix} u_{k^-} \\ v_{k^-} \end{pmatrix} e^{ik^-x} \right) e^{ik_y y} \quad (2.6)$$

$$\psi_{S(h)}(x, y) = \left( \bar{c}_1 \begin{pmatrix} u_{k^+} \\ v_{k^+} \end{pmatrix} e^{-ik^+x} + \bar{d}_1 \begin{pmatrix} u_{-k^-} \\ v_{-k^-} \end{pmatrix} e^{ik^-x} + \bar{c}_2 \begin{pmatrix} u_{-k^+} \\ v_{-k^+} \end{pmatrix} e^{ik^+x} + \bar{d}_2 \begin{pmatrix} u_{k^-} \\ v_{k^-} \end{pmatrix} e^{-ik^-x} \right) e^{ik_y y} \quad (2.7)$$

where the plus and minus signs in the superscripts of the wave vectors refer to electron-like and hole-like excitations, respectively.  $c_1$ ,  $\bar{c}_1$  and  $d_1$ ,  $\bar{d}_1$  are the electron-like and hole-like quasiparticle transmission coefficients, respectively.  $c_2$ ,  $c_2$  and  $d_2$ ,  $d_2$  are electron-like and hole-like quasiparticle reflection coefficients, respectively.

Similar to that of the metal on the left, the excitation energy spectrum of the metal on the right region ( $x > L$ ) are

$$E_{MR} = \pm \frac{\hbar^2 (q_R^2 + k_y^2)}{2m} \mp E_{FR} \quad (2.8)$$

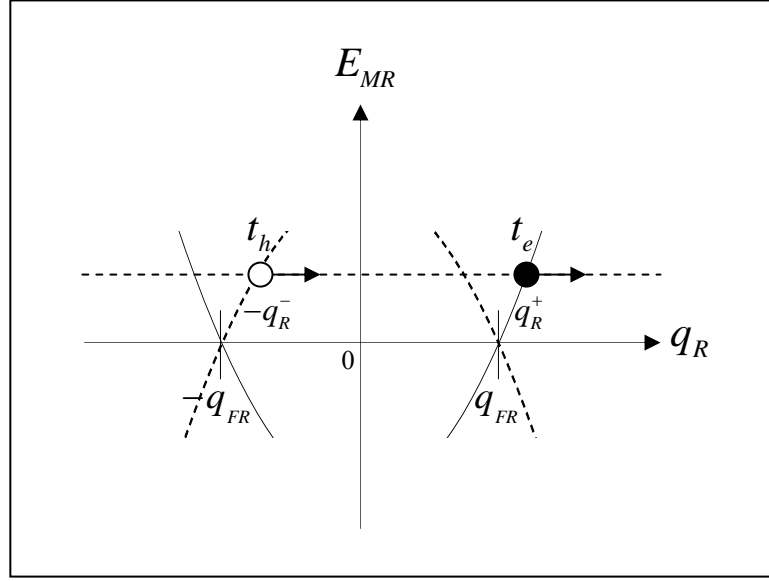


**Figure 2.5** The diagram of the excitation energy dispersion relation of the particles in the metal on the right. The black and white dots represent the transmitted excited electron and excited hole in the case where an electron is injected from the left side, respectively.

The wave functions of the excitations in the metal on the right in both cases of injections are

$$\psi_{MR(e)}(x, y) = \left( t_e \begin{pmatrix} 1 \\ 0 \end{pmatrix} e^{iq_R^+ x} + t_h \begin{pmatrix} 0 \\ 1 \end{pmatrix} e^{-iq_R^- x} \right) e^{ik_y y} \quad (2.9)$$

$$\psi_{MR(h)}(x, y) = \left( \begin{pmatrix} 0 \\ 1 \end{pmatrix} e^{iq_R^- x} + \bar{r}_h \begin{pmatrix} 0 \\ 1 \end{pmatrix} e^{-iq_R^- x} + \bar{r}_e \begin{pmatrix} 1 \\ 0 \end{pmatrix} e^{iq_R^+ x} \right) e^{ik_y y} \quad (2.10)$$

where  $t_e$  and  $t_h$  are the excited electron and excited hole transmission coefficients, respectively.  $\bar{r}_h$  and  $\bar{r}_e$  are the normal and the Andreev reflection coefficients,

respectively.  $q_R^+$  and  $q_R^-$  are the  $x$ -component of the wave vectors of the excited electron and hole in the metal on the right hand side, respectively.

In this approach, the current and conductance are obtained through the transmission and reflections probabilities. We thus have to compute for all the transmission and reflection amplitudes from a set of equations referred to as appropriate matching conditions at each interface. The first set of matching equations is obtained from the fact that the wave functions are continuous at both interfaces, whereas the second one is obtained from the discontinuity of the slopes of wave functions at both interfaces due to the delta-function potentials representing the insulating layers. That is,

$$\psi_{ML}(x = 0) = \psi_S(x = 0) \quad (2.11)$$

$$\psi_{MR}(x = L) = \psi_S(x = L) \quad (2.12)$$

$$\frac{d\psi_S}{dx}(x = 0) - \frac{d\psi_{ML}}{dx}(x = 0) = 2k_F Z_1 \psi_{ML}(x = 0) \quad (2.13)$$

$$\frac{d\psi_{MR}}{dx}(x = L) - \frac{d\psi_S}{dx}(x = L) = 2k_F Z_2 \psi_{MR}(x = L) \quad (2.14)$$

where  $Z_1 = mH_1/\hbar k_F^2$  and  $Z_2 = mH_2/\hbar k_F^2$  are the unitless parameters characterizing the barrier strengths at left and right interfaces of a junction, respectively.

From these equations, we can obtain the particle reflection and transmission coefficients, which we then use to calculate the corresponding particle transmission and reflection probabilities. From quantum mechanics the particle reflection or transmission probability is defined as the ration of the reflected or transmitted particle

current density and the incoming particle current density (Shankar, 1994). Thus, the Andreev reflection probabilities in both cases of injection are

$$R_h(E, \theta) = \left| \frac{j_{refl(\bar{r}_h)}}{j_{inc}} \right| = \left| r_h(E, \theta) \right|^2 \left( \frac{q_{ML}^-}{q_{ML}^+} \right) \quad (2.15)$$

and

$$\bar{R}_e(E, \theta) = \left| \frac{j_{refl(\bar{r}_e)}}{j_{inc}} \right| = \left| \bar{r}_e(E, \theta) \right|^2 \quad (2.16)$$

The normal reflection probabilities in both cases of injection are

$$R_e(E, \theta) = \left| \frac{j_{refl(r_e)}}{j_{inc}} \right| = \left| r_e(E, \theta) \right|^2 \quad (2.17)$$

and

$$\bar{R}_h(E, \theta) = \left| \frac{j_{refl(\bar{r}_h)}}{j_{inc}} \right| = \left| \bar{r}_h(E, \theta) \right|^2 \left( \frac{q_{ML}^+}{q_{MR}^-} \right) \quad (2.18)$$

The electron-like quasiparticle transmission probabilities in both cases of injection are

$$T_e(E, \theta) = \left| \frac{j_{trans(t_e)}}{j_{inc}} \right| = \left| t_e(E, \theta) \right|^2 \left( \frac{q_{MR}^+}{q_{ML}^+} \right) \quad (2.19)$$

and

$$\bar{T}_e(E, \theta) = \left| \frac{j_{trans(\bar{t}_e)}}{j_{inc}} \right| = \left| \bar{t}_e(E, \theta) \right|^2 \left( \frac{q_{ML}^+}{q_{MR}^-} \right) \quad (2.20)$$

The hole-like quasiparticle transmission probabilities in both cases of injection are

$$T_h(E, \theta) = \left| \frac{j_{trans(t_h)}}{j_{inc}} \right| = \left| t_h(E, \theta) \right|^2 \left( \frac{q_{MR}^-}{q_{ML}^+} \right) \quad (2.21)$$

and

$$\bar{T}_h(E, \theta) = \left| \frac{j_{trans(\bar{t}_h)}}{j_{inc}} \right| = \left| \bar{t}_h(E, \theta) \right|^2 \left( \frac{q_{ML}^-}{q_{MR}^-} \right) \quad (2.22)$$

In each case of injection, at each interface the total incoming probabilities are equal to the total outgoing probabilities due to the conservation of the number of particle current.



The electric current density flowing to the right ( $I$ ) is defined as

$$I = \sum_{kx,ky} n_k v_k e \quad (2.23)$$

where  $n_k$  is number of electron moving from left to right across the junctions,  $v_k$  is the group velocity, and  $e$  is the electron charge.  $n_k$  is equal to  $n_k = (1 + R_h(E, \theta) - R_e(E, \theta) + \bar{T}_e(E, \theta) - \bar{T}_h(E, \theta))f(E)$ , where  $f(E)$  is the Fermi-Dirac distribution function. Because there is no net current flowing across the junction when there is no applied voltage, we can assume that there is an equal amount of electric current density flowing to from right to left as well. By changing the summation over the momenta along  $x$  and  $y$  direction to the integral over the momenta along  $y$  direction and the energy, we have

$$I_{L \rightarrow R} = I_{R \rightarrow L} = \frac{e}{\hbar} \left( \frac{L}{2\pi} \right)^2 \int_{-\infty}^{\infty} \int_{-\infty}^{\infty} dk dE (1 + \bar{R}_h(E, \theta) - \bar{R}_e(E, \theta) + T_e(E, \theta) - T_h(E, \theta)) f(E) \quad (2.24)$$

When the voltage  $V$  is applied across the junction, the electric current flowing across junctions from left to right becomes, while that flowing from right to left stays the same. That is,

$$I_{L \rightarrow R} = \frac{e}{\hbar} \left( \frac{L}{2\pi} \right)^2 \int_{-\infty}^{\infty} \int_{-\infty}^{\infty} dk dE (1 + R_h(E, \theta) - R_e(E, \theta) + \bar{T}_e(E, \theta) - \bar{T}_h(E, \theta)) f(E - eV) \quad (2.25)$$

and

$$I_{R \rightarrow L} = \frac{e}{\hbar} \left( \frac{L}{2\pi} \right)^2 \int_{-\infty}^{\infty} \int_{-\infty}^{\infty} dk dE (1 - \bar{R}_h(E, \theta) + \bar{R}_e(E, \theta) + T_e(E, \theta) - T_h(E, \theta)) f(E) \quad (2.26)$$

Therefore, the net current crossing the junctions is

$$I(eV, \theta) = I_{L \rightarrow R} - I_{R \rightarrow L} \quad (2.27)$$

$$I(eV, \theta) = \frac{e}{\hbar} \left( \frac{L}{2\pi} \right)^2 \int_{-\infty}^{\infty} \int_{-\infty}^{\infty} dk dE [(1 + R_h(E, \theta) - R_e(E, \theta) + \bar{T}_e(E, \theta) - \bar{T}_h(E, \theta))(f(E - eV) - f(E))] \quad (2.28)$$

Since  $k_y = k_F \sin \theta$  and then  $dk_y = k_F \cos \theta d\theta$

$$I(eV, \theta) = \frac{ek_F}{\hbar} \left( \frac{L}{2\pi} \right)^2 \int_{-\pi/2}^{\pi/2} d\theta \cos \theta \int_{-\infty}^{\infty} dE [(1 + R_h(E, \theta) - R_e(E, \theta) + \bar{T}_e(E, \theta) - \bar{T}_h(E, \theta))(f(E - eV) - f(E))] \quad (2.29)$$

At zero temperature, the net current becomes

$$I(eV, \theta) = \frac{ek_F}{\hbar} \left( \frac{L}{2\pi} \right)^2 \int_{-\pi/2}^{\pi/2} d\theta \cos \theta (1 + R_h(E, \theta) - R_e(E, \theta) + \bar{T}_e(E, \theta) - \bar{T}_h(E, \theta)) eV \quad (2.30)$$

The conductance at zero temperature is therefore

$$G(eV, \theta) = \frac{dI(eV, \theta)}{dV} \quad (2.31)$$

$$G(eV, \theta) = \left( \frac{Le}{2\pi\hbar} \right)^2 \int_{-\pi/2}^{\pi/2} d\theta k_F \cos \theta (1 + R_h(E, \theta) - R_e(E, \theta) + \bar{T}_e(E, \theta) - \bar{T}_h(E, \theta)) \quad (2.32)$$

In the next chapter, we will present the results and discussion of our calculation for both s-wave and d-wave cases.

# CHAPTER III

## CONDUCTANCE SPECTRA OF MSM JUNCTIONS

In this chapter, we show and discuss the results of our calculation of the conductance in both s-wave and d-wave cases. We reconsider effects of the thickness of superconducting layer  $L$ , i.e. the Tomasch oscillations, and explore the influence of the heights of the barrier potentials representing by the parameters  $Z_1$  and  $Z_2$  in both cases of the superconducting gap. Also, because in d-wave cases the superconducting gap is anisotropic, we consider the effect of the crystal orientation on the conductance spectrum as well.

### 3.1 The effect of the thickness of superconducting layer

In the s-wave case, the thickness of superconducting layer affects of the oscillations in the conductance spectra. To be more specific, in the  $eV < \Delta_0$  region, the conductance spectra do not contain any oscillations. However, the height of the peak at the energy gap is increased with the thickness. In the  $eV > \Delta_0$  region, the oscillations of conductance spectra occur and strongly depend on  $L$ . The period of the oscillations is decreased with the increased in  $L$ , as shown in Figure 3.1.

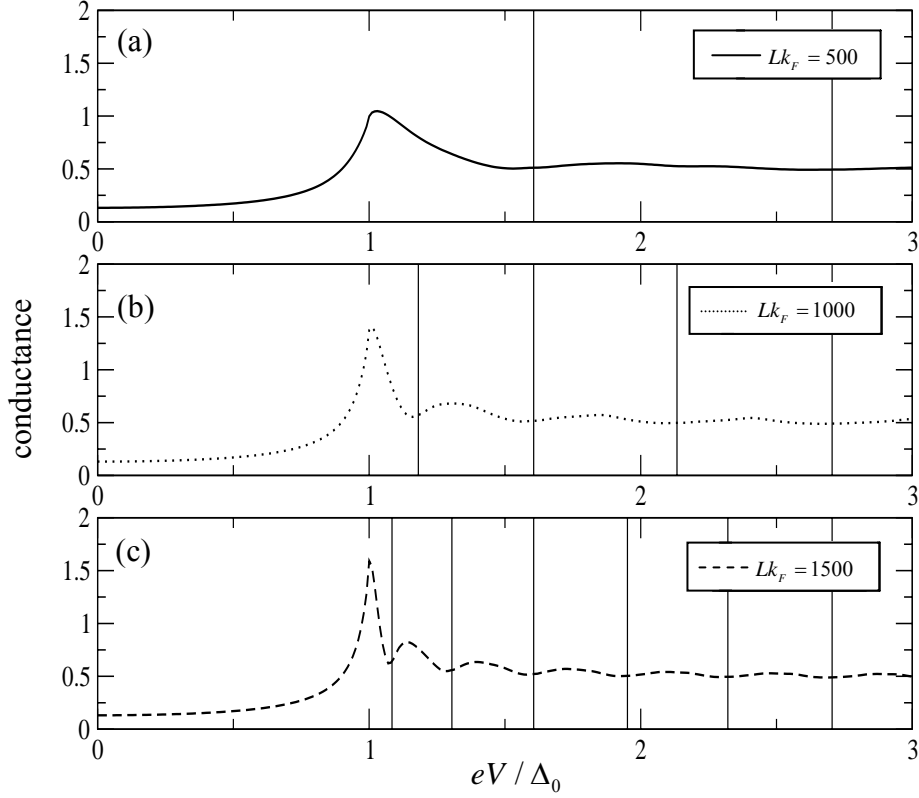


**Figure 3.1** The conductance as a function of applied voltage ( $eV/\Delta_0$ ) for three different thicknesses of the s-wave superconducting layer ( $Lk_F$ ): (a)  $Lk_F = 500$ , (b)  $Lk_F = 1000$ , and (c)  $Lk_F = 1500$ . Here,  $\Delta_0/E_F = 0.01$  and  $Z_1 = Z_2 = 1.0$ . The solid upright lines represent the positions of the minima of the oscillations in the conductance spectra.

In the case of a d-wave superconductor, unlike in the s-wave case, it is found that in the  $eV < \Delta_0$  region, oscillations with small amplitudes can occur. They are more prominent when the superconducting layer is thicker. These oscillations are caused by the fact that the amplitude of a d-wave gap is not constant and oscillations in all reflection and transmission probabilities can occur at all energies. In the

$eV > \Delta_0$  region, the conductance spectra contain similar oscillations to those in the s-wave case, as shown in Figure 3.2.

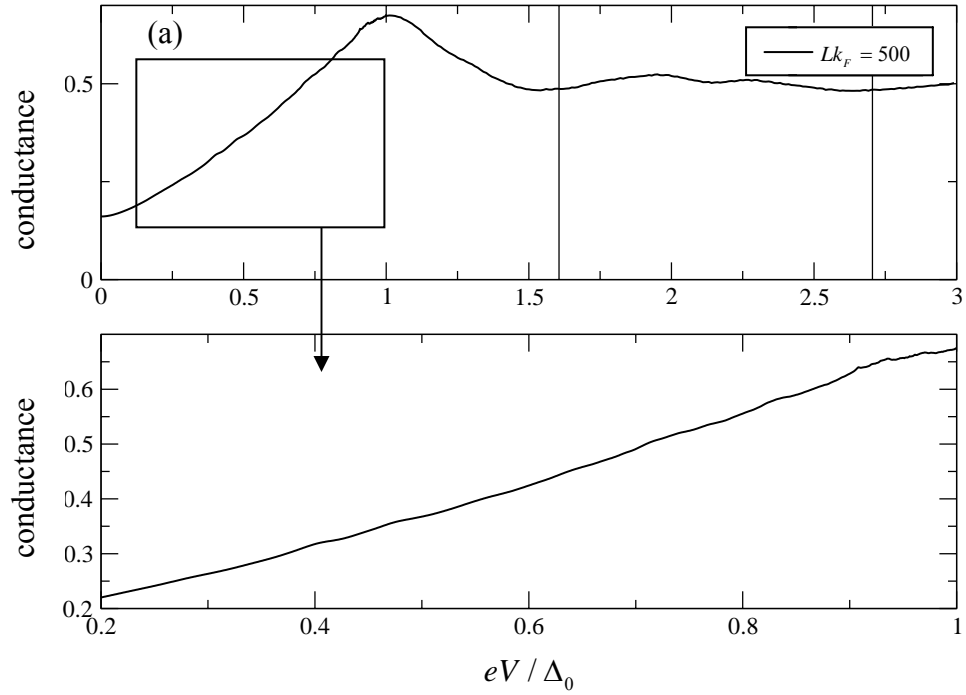


**Figure 3.2** The conductance as a function of applied voltage ( $eV/\Delta_0$ ) for three different thicknesses of the d-wave superconducting layer ( $Lk_F$ ): (a)  $Lk_F = 500$ , (b)  $Lk_F = 1000$ , and (c)  $Lk_F = 1500$ . Here,  $\Delta_0/E_F = 0.01$ ,  $Z_1=Z_2=1.0$ , and  $\alpha = 0$ . The solid upright lines represent the positions of the minima of the oscillations in the conductance spectra.

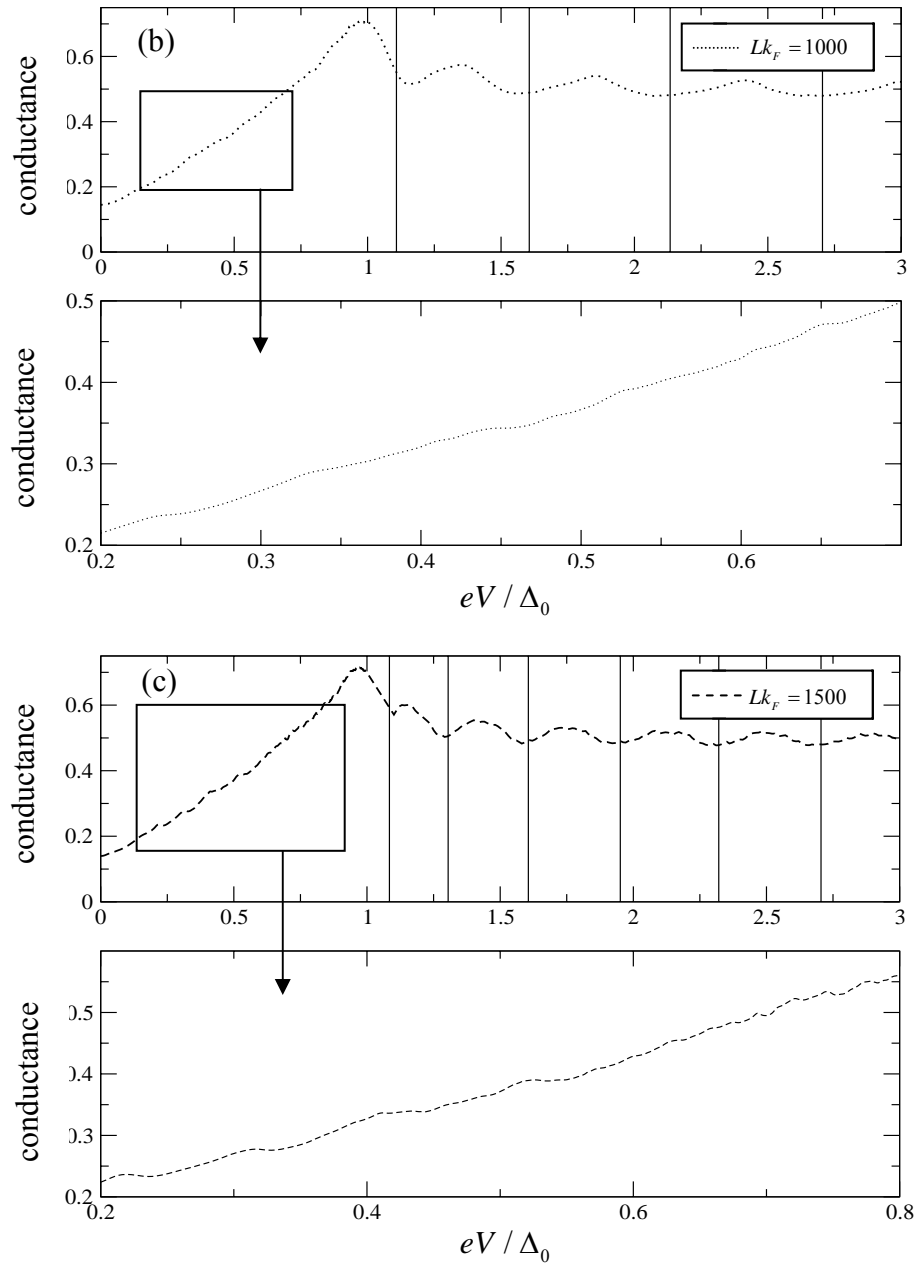


**Figure 3.2** The conductance as a function of applied voltage ( $eV/\Delta_0$ ) for three different thicknesses of the d-wave superconducting layer ( $Lk_F$ ): (a)  $Lk_F = 500$ , (b)  $Lk_F = 1000$ , and (c)  $Lk_F = 1500$ . Here,  $\Delta_0/E_F = 0.01$ ,  $Z_1=Z_2 = 1.0$ , and  $\alpha = 0$ . The solid upright lines represent the positions of the minima of the oscillations in the conductance spectra. (Continued)

As shown by McMillan and Anderson (1996), the peak of these oscillations correspond to the excitation energy levels of the quasiparticles in the superconducting layer:

$$E_n = \sqrt{\left(\frac{2n\pi E_F}{k_F L \cos \theta_k}\right)^2 + \Delta_k^2} \quad (2.32)$$

where  $n = 1, 2, 3, \dots$ , and  $E_n$  is the position of each oscillation peak. Our results are consistent with this finding, that is, the position of  $E_n$  coincide with the minima of the oscillations in the conductance spectra.

### 3.2 The effect of insulating barrier potentials

In this section, we examine the effect of the insulating barrier potentials, which are characterized by the parameters  $Z_1$  and  $Z_2$ . First, we consider the case where both potentials are equal and later on the case where they are unequal.

When  $Z_1$  and  $Z_2$  are equal, in both s-wave and d-wave cases we find that the overall conductance spectra are suppressed as  $Z_1$  and  $Z_2$  are increased, as shown in Figure 3.3 (a) and (b). The barrier potentials do not affect the oscillation period. They however reduce the probabilities of particle transmission and hence the decrease in the conductance.

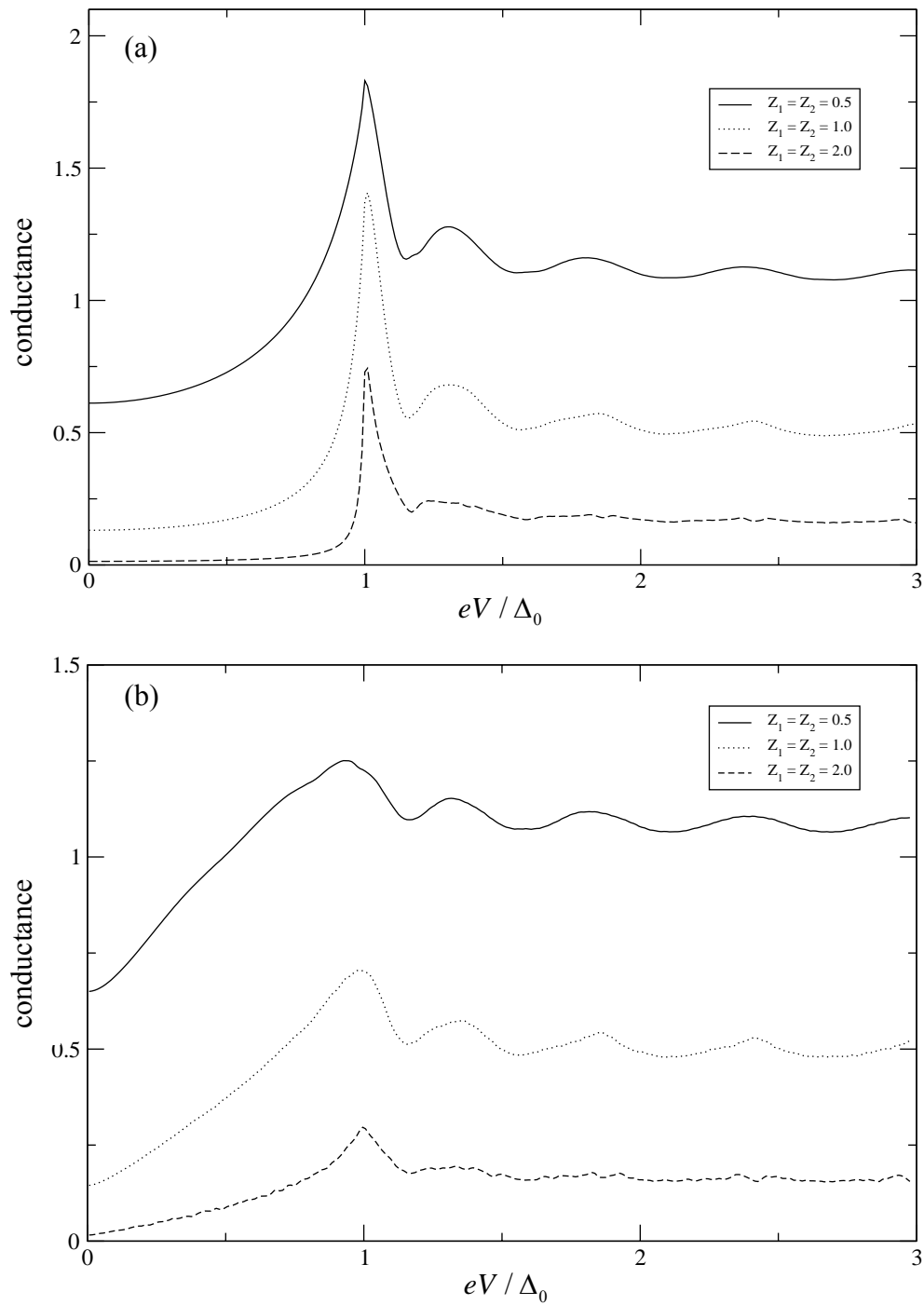


**Figure 3.3** The conductance spectra of MSM junctions with the different values of  $Z_1$  and  $Z_2$ . Here, we take  $\Delta_0 / E_F = 0.01$  and  $Lk_F = 1000$ : (a) s-wave case and (b) d-wave case.



When  $Z_1$  and  $Z_2$  are unequal, things are more interesting. In the s-wave case, when  $Z_1$  is fixed, the variation of  $Z_2$  does not affect the conductance spectra in the  $eV < \Delta_0$  region, whereas the conductance spectra in the  $eV > \Delta_0$  region is very much affected. That is, the spectra in this region are suppressed by the increase in  $Z_2$  as shown in Figure 3.4.

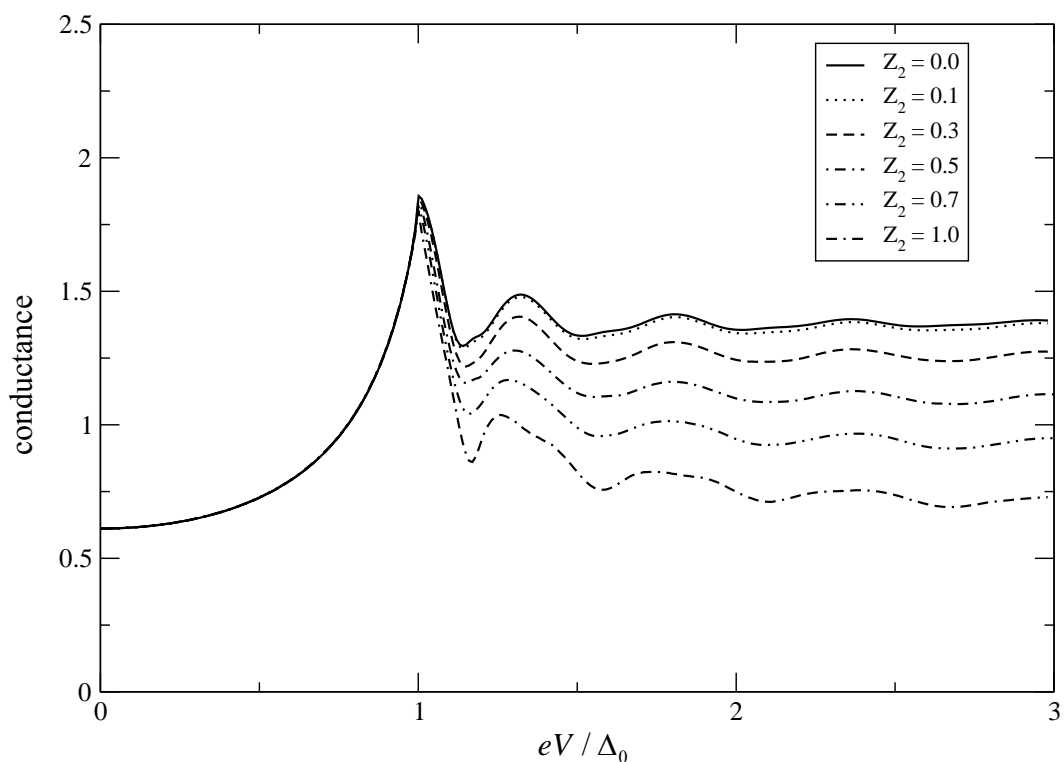


**Figure 3.4** The conductance spectra of s-wave superconductor with different values of  $Z_2$ . We take  $\Delta_0 / E_F = 0.01$ ,  $Lk_F = 1000$ , and  $Z_1 = 0.5$ .

In case of a d-wave superconductor, the overall spectra are affected by the change in  $Z_2$ . The effect of  $Z_2$  on the conductance spectrum in the  $eV < \Delta_0$  region of a d-wave junction is more than that of an s-wave junction due to the gap anisotropy.

In the  $eV > \Delta_0$  region, the conductance spectrum is affected in the same way as in the s-wave case. Again, the oscillation period is not affected by the change in the barrier

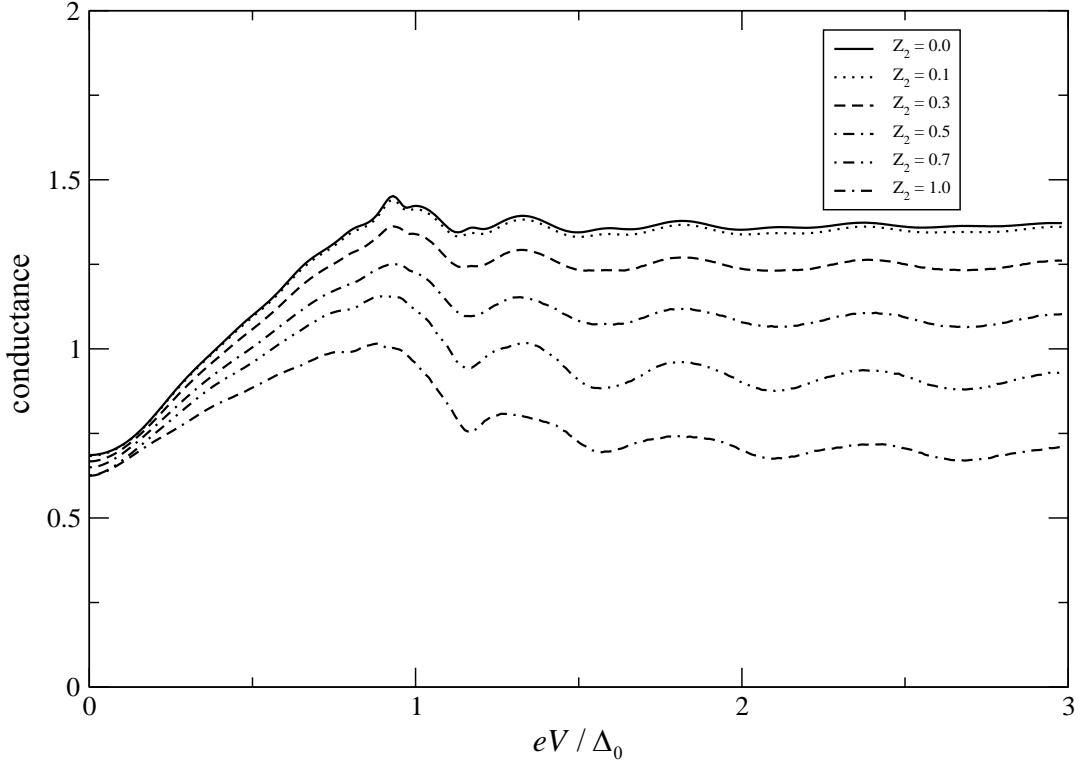


**Figure 3.5** The conductance spectra of d-wave superconductor with different values of  $Z_2$ . We take  $\Delta_0 / E_F = 0.01$ ,  $Lk_F = 1000$ ,  $\alpha = 0$ , and  $Z_1 = 0.5$ .

When  $Z_2$  is fixed, one can see that, in both s-wave and d-wave cases as shown in Figures 3.6 and 3.7, respectively, the overall conductance spectra are influenced by  $Z_1$  more dramatically than in the case we considered above. This difference can be used to distinguish the quality of the two interfaces of MSM double junctions.

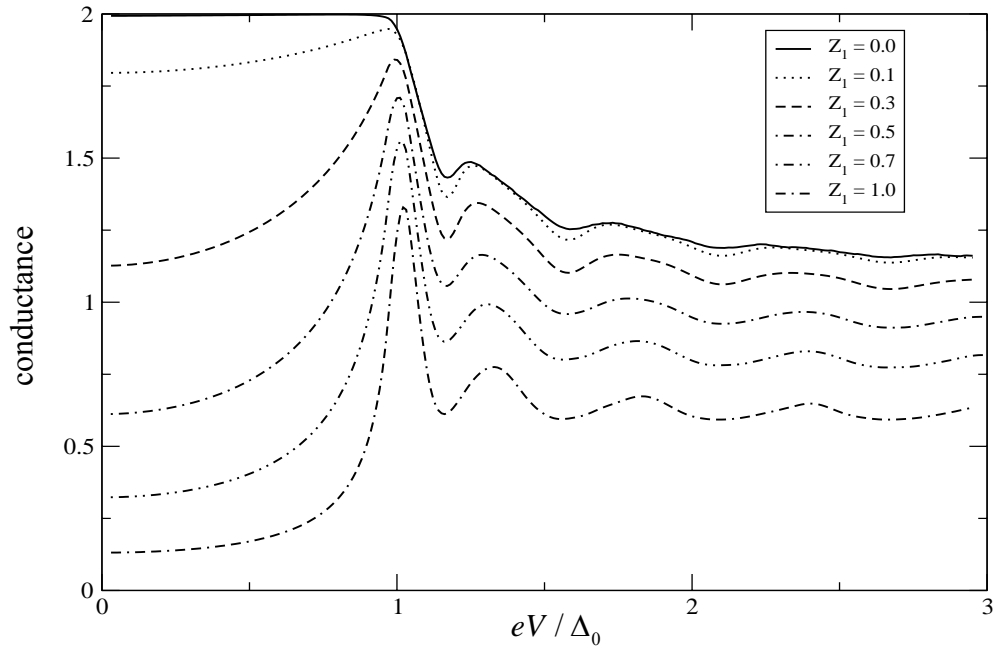


**Figure 3.6** The conductance spectra of s-wave superconductor with different values of  $Z_2$ . We take  $\Delta_0 / E_F = 0.01$ ,  $Lk_F = 1000$ , and  $Z_2 = 0.7$ .

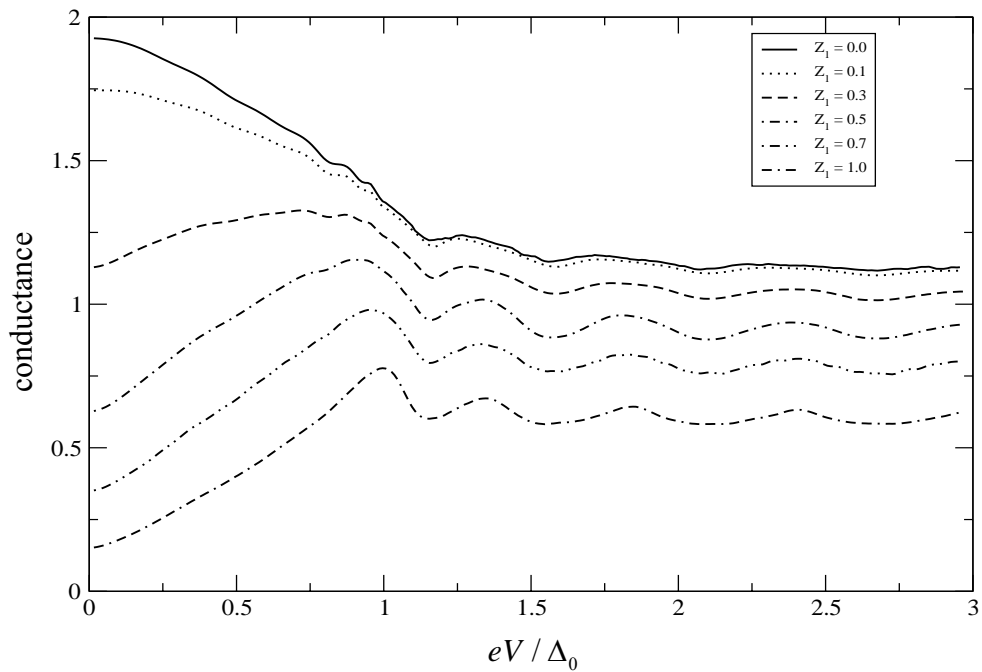


**Figure 3.7** The conductance spectra of d-wave superconductor with different values of  $Z_2$ . We take  $\Delta_0 / E_F = 0.01$ ,  $Lk_F = 1000$ ,  $\alpha = 0$ , and  $Z_2 = 0.7$ .

### 3.3 The effect of the crystal orientation of d-wave superconductor

Now we consider the influence of the crystal orientation of a d-wave superconductor on the conductance spectrum of the double junction. The orientation is characterized by the parameter  $\alpha$ , the angle between the  $a$ -axis of the crystal of the d-wave superconductor and the interface normal of the interface. As can be seen in Figure 3.8, the crystal orientation of the d-wave superconductor has a very strong effect on the whole range of the conductance spectrum. There is a zero-bias conductance peak (ZBCP) developing as  $\alpha$  is increased from 0 to  $\pi/4$ . Specifically, there is no ZBCP when  $\alpha = 0$ . As  $\alpha$  is increased, the ZBCP starts to appear. Its height and width are increased as  $\alpha$  approaches  $\pi/4$ . The period of the oscillations in the conductance spectrum is also affected by the change in  $\alpha$ .

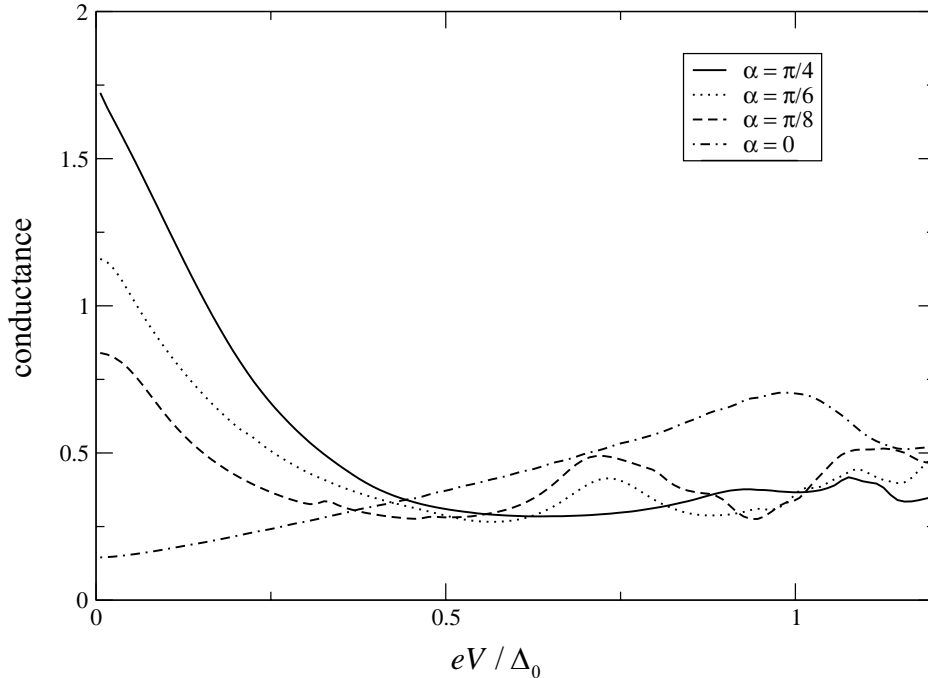


**Figure 3.8** The conductance spectra of d-wave junctions with different values of  $\alpha$ : 0,  $\pi/8$ ,  $\pi/6$ , and  $\pi/4$ . We take  $\Delta_0 / E_F = 0.01$  and  $Z_1 = Z_2 = 1$ .

## CHAPTER IV

### CONCLUSIONS

We have theoretically investigated the conductance spectra of metal-superconductor-metal (MSM) junctions, where the superconducting layer is either isotropic s-wave or d-wave. We use a scattering method to obtain the particle transmission and reflection probabilities, which are then used to calculate the electric current across an MSM junction as a function of the applied voltage. As is already well understood, changes in thickness of the superconducting layer give rise to oscillatory behavior in the conductance spectra, which are known as the Tomasch oscillations. The effect results the interference of waves scattered from the two boundaries of the superconducting layer (Tomasch, 1966 and Tomasch and Wolfram, 1966). These oscillations contained detailed information about the material properties of the superconductor and the metals in the junction. In particular, they can be used to extract the Fermi velocity ( $v_F$ ) and the energy gap of the superconductor (McMillan and Anderson, 1966).

The effect of a variation in the relative barrier heights at the two metal-superconductor interfaces on the conductance spectrum was our main focus in both cases of s-wave and d-wave gap symmetry. We found that the left (high voltage) and right (low voltage) barrier heights affect the conductance spectrum in a different way. In particular, the size of the left barrier (i.e. the barrier to incident electrons) determines the shape of the conductance across the entire range of the applied voltage.

As the left barrier increases, spectral features of the conductance are suppressed, resulting in an overall decrease in conductance. The right barrier (the barrier to incident holes) hardly affects the conduction spectrum, when the applied voltage is smaller than the maximum gap. An increase in the height of the right barrier only affects the spectrum when the applied voltage is larger than the maximum gap. It decreases the conductance in this range.

In addition to the effect of the two barriers, when we studied MSM junctions with d-wave superconductors, we also focus on the orientation-dependence of the conductance, we asked: how does the conductance spectrum depend on the angle between the superconductor crystal axis and the normal to the metal-superconductor interface?

The band structure of our simple model of the superconductor is isotropic, so all orientation dependence came from the anisotropic superconducting gap. The d-wave gap (which is known to occur in high-temperature superconductors and other materials) vanishes along two perpendicular directions the nodal directions in the two dimensional momentum space.

When the normal to the junction interface is parallel to the nodal direction, along which the gap vanishes, the conductance spectrum shows a prominent peak centered at zero voltage, similar to a single metal-d-wave superconductor junction (Tanaka and Kashiwaya, 1995). As the superconductor is rotated, this peak is suppressed. When the junction interface normal is parallel to the direction along which the gap is maximum (and thus makes a  $45^\circ$  angle with the nodal direction) this

zero-voltage peak is absent. Other features of the conductance spectrum show a similarly strong dependence on crystal orientation, as discussed in detail above.

In conclusion, we have identified new dependences of the MSM conductance spectrum on properties of the constituent materials. For s-wave superconductors, we have found that, depending on the range of applied voltage, one interface or the other (i.e. the high or low potential interface) dominates the conductance whereas the other plays a lesser role. This finding would allow experimentalists to isolate barrier effects involving two different metals by varying the voltage in order to disentangle the effects of the two interfaces. For d-wave superconductors we have detailed the dependence of the conductance on the junction orientation extending previous work by including all intermediate angles (previous studies typically concentrated on cases where the interface normal was either parallel to the nodal direction or the maximum-gap direction). This could help experimentalists interpret results when the exact orientation of the interface is difficult to determine or control.

## **REFERENCES**



## REFERENCES

- Blonder, G. E., Tinkham, M., and Klapwijk, T. M. (1982). Transition from metallic to tunneling regimes in superconducting microconstrictions: Excess current, charge imbalance, and supercurrent conversion. **Phys. Rev. B** 25(7): 4515-4532.
- Dong, Z. C., Zheng, Z. C., and Xing, D. Y. (2004). Coherent tunneling conductance in normal-metal/d-wave superconductor/normal-metal double tunnel junctions. **J. Phys.:Condens. Matter** 16(34): 6099-6108.
- Griffin, A. and Demers, J. (1971). Tunneling in the normal-metal-insulator-superconductor geometry using the Bogoliubov equations of motion. **Phys. Rev. B** 4(7): 2202-2208.
- Koren, G., Polturak, E., and Deutscher, G. (1996). Oxygen controlled transition from tunneling to a weak link behavior in  $\text{YBa}_2\text{Cu}_3\text{O}_{7-\delta}/\text{Ba}_2\text{CoCu}_2\text{O}_y/\text{YBa}_2\text{Cu}_3\text{O}_{7-\delta}$  wedge edge junctions. **Physica C** 259: 379-384.
- Lykken, G. I., Geiger, A. L., Dy, K. S., and Mitchell, E. N. (1970). Measurement of the Fermi velocity in single-crystal films of lead by electron tunneling. **Phys. Rev. Lett.** 25(22): 1578-1580.
- Lykken, G. I., Geiger, A. L., Dy, K. S., and Mitchell, E. N. (1971). Measurement of the superconducting energy gap and Fermi velocity in single-crystal lead films by electron tunneling. **Phys. Rev. B** 4(5): 1523-1530.

- Marder, M. (2000), **Condensed matter physics**. New York: John Wiley and Sons.
- McMillan, W. L. and Anderson, P. W. (1966). Theory of geometrical resonances in the tunneling characteristics of thick films of superconductors. **Phys. Rev. Lett.** 16(3): 85-87.
- Nesher, O. and Koren, G. (1999). Observation of Tomasch oscillations and tunneling-like behavior in oxygen-deficient edge junctions. **Appl. Phys. Lett.** 74(22): 3392-3394.
- Tanaka, Y. and Kashiwaya, S. (1995). Theory of tunneling spectroscopy of d-wave superconductors. **Phys. Rev. Lett.** 74(17): 3451-3454.
- Tomasch, W. J. (1965). Geometrical resonance in the tunneling characteristics of superconducting Pb. **Phys. Rev. Lett.** 15(16): 672-675.
- Tomasch, W. J. (1966). Geometrical resonance and boundary effects in tunneling from superconducting In. **Phys. Rev. Lett.** 16(1): 16-19.
- Tomasch, W. J. and Wolfram, T. (1966). Energy spacing of geometrical resonance structure in very thick films of superconducting In. **Phys. Rev. Lett.** 16(9): 352-354.
- Tsuei, C. C. and Kirtley, J. R. (2000). Pairing symmetry in cuprate superconductors. **Rev. Mod. Phys.** 72(4): 969-1016.
- Shankar, R. (1994). **Principles of quantum mechanics (2nd edition)**. Berlin: Springer.

# CURRICULUM VITAE

Miss Areerat Dawongsa

Date of birth: July 25, 1982

Place of birth: Loei, Thailand

Nationality: Thai

## **Education**

Academic year

2001-2005 Bachelor of Science (Physics)

Loei Rajabhat University, Loei, Thailand.